Quasineutral PIC Electron Guiding Center modeling in the presence of slow cross-field electron transport in a Hall thruster

IEPC-2013-286

Presented at the 33rd International Electric Propulsion Conference,
The George Washington University, Washington, D.C., USA
October 6–10, 2013

Dariusz Daniłko* and Serge Barral†
Institute of Plasma Physics and Laser Microfusion, Hery 23, 01-497 Warsaw, Poland

and

Stéphan Zurbach‡
Snecma, Safran Group, 27208 Vernon, France

A one-dimensional cross-field electron transport solver for a 2D Particle-In-Cell (PIC) code with guiding center approximation for electrons and Monte-Carlo collisions is developed. An original approach based on a random walk is adopted to describe the transport of the guiding centers. This approach significantly simplifies the computation of the cross-field electron transport.

Nomenclature

t	=	time
r	=	coordinate in the radial direction
z	=	coordinate in the axial direction
y	=	coordinate in the azimuthal direction
x	=	coordinate in the direction perpendicular to B in the r-z plane
ζ	=	coordinate along the magnetic field
B	=	magnetic field
A	=	magnetic potential
E	=	electric field
$E_\parallel$	=	electric field parallel to the magnetic field
$E_\perp$	=	electric field perpendicular to the magnetic field
Φ	=	electric potential
e	=	elementary charge = $1.602176465 \times 10^{-19}$ C
q_e	=	electron charge = $-e$
q_i	=	ion charge = $+e$ for Xe^+
m_e	=	electron mass = $9.10938188 \times 10^{-31}$ kg
m_i	=	ion mass = $2.18017136555 \times 10^{-25}$ kg (for Xenon)

*Assistant, Division of Magnetised Plasma, dariusz.danilko@ipplm.pl
†Research Scientist, Division of Magnetised Plasma, serge.barral@ipplm.pl
‡R & D Engineer, Space Engines Division, stephan.zurbach@snecma.fr

N_e	=	number of electrons
n_e	=	electron number density
n_i	=	ion number density
n_n	=	number density of neutral gas
$v_{e_\parallel}$	=	electron velocity parallel to the magnetic field
$v_{e_\perp}$	=	electron velocity perpendicular to the magnetic field
v_x	=	x component of the electron velocity
v_y	=	y component of the electron velocity
$T_{e_\parallel}$	=	electron temperature parallel to the magnetic field
$T_{e_\perp}$	=	electron temperature perpendicular to the magnetic field
μ	=	electron magnetic moment = $\frac{v_{e_\perp}^2}{2B}$
ω_c	=	electron gyrofrequency
ν_e	=	electron collision frequency
ω_{pe}	=	plasma frequency
ρ	=	charge density
k_B	=	Boltzmann's constant = $1.3806488 \times 10^{-23}$ J/K
ε_0	=	permittivity of the free space = 8.85419×10^{-12} F/m
σ_{max}	=	maximum cross section of a given collision type
$\mathcal{P}_{collision}$	=	collision probability
x_{gc}	=	coordinate of the guiding center in direction of $E_\perp$
x_c	=	coordinate of the collision point in direction of $E_\perp$

Introduction

THE aim of this work is to develop a cross-field electron transport solver for a 2D (r-z) kinetic code with guiding center approximation for electrons. This approximation allows for the use of time steps much longer than the electron gyroperiod and spatial resolution coarser than the electron Larmor radius. The purpose of using the guiding center approximation is to make the code significantly faster than fully kinetic codes and more accurate than codes using a fluid or a hybrid approach. The biggest gain compared to codes treating electrons as fluid is that no assumptions regarding electron distribution have to be made, which makes it possible to model subtle kinetic effects.

The code being developed is a 2D3V Particle-In-Cell (PIC) model with three particle species: neutrals, unmagnetized ions and electrons described by their guiding centers, which effectively reduces dimension of the phase space to four. A Monte-Carlo method is employed to account for particle-particle collisions. Macroscopic quantities are computed on a two-dimensional (r-z) field-aligned computational grid.

In order to integrate the equations for electron motion, we first decompose a 2D grid into a set of 1D subgrids aligned with the radial magnetic field lines. This decomposition exploits the fact that the characteristic velocity of electrons along the magnetic field line is much faster than any other velocity in the model, particularly the one connected with the cross-field electron transport.

Each of the 1D subgrids is treated as a separate subsimulation governed by a 1D model based on the code by Miedzik et al. [1, 2]. The momentum conservation equation governs the motion of electron guiding center along the magnetic field:

$$\frac{\partial v_{e_\parallel}}{\partial t} = \frac{q_e}{m_e} E_\parallel - \mu \frac{\partial B}{\partial \zeta} \ . \tag{1}$$

Electrons are advanced in time using a Semi Implicit MidPoint (SIMP) scheme [3].

The electric field along the magnetic field is calculated using the following formula [1]:

$$q_e E_\parallel = \frac{B}{n_i} \frac{\partial}{\partial \zeta} \left(\frac{n_i k_B T_{e_\parallel}}{B} \right) - \langle \mu \rangle \frac{\partial B}{\partial \zeta} \ . \tag{2}$$

Here $\langle \mu \rangle$ is the mean magnetic moment of electrons. In Eq. (2) the electron number density was replaced by the ion number density in order to ensure quasineutrality [4].

In order to create a 2D code we need to enable communication between each of the 1D subsimulation in terms of cross-field particle transport. Ion and neutral cross-field transport solvers are straightforward to implement as neither of the species is magnetized. Electrons, however, are attributed to specific magnetic lines until they experience a collision. Their motion along the axis of the thruster is best described in terms of the random walk theory. The authors are not aware of earlier work regarding the transport of electrons described in the frame of the guiding center approximation in the direction perpendicular to the magnetic field.

A one-dimensional model (z) has been developed in order to find a suitable cross-field electron transport solver for the 2D simulation. The code models three particle species: monokinetic neutrals, ions and electrons described with a guiding center approximation. The regular computational grid extends from the anode to the cathode and is permeated by an arbitrary radial magnetic field. The boundary conditions are the following:

ANODE: all electrons reaching the anode are absorbed; all ions are recombined, creating a neutral atom; neutral gas is injected at a constant mass flow rate.

CATHODE: all particles reaching the cathode leave the simulation region; additionally the cathode injects enough electrons to maintain quasineutrality in the adjacent numerical cell.

I. Particle collisions in the (x-y) space

The code accounts for three types of electron-neutral interactions: ionization, excitation and scattering. The momentum transfer between a neutral particle and an electron is negligibly small and is not taken into account in the computations.

A. Monte Carlo method

All particle collisions are performed in the frame of Monte Carlo methodology and use a null collision approach [5]. Having cross section data for a given type of particle interaction, we first determine the maximum number of particles, N, that may undergo a certain type of collision in a given timestep:

$$N = \mathcal{P}_{max} N_e, \tag{3}$$

$$\mathcal{P}_{max} = 1 - e^{-n_n \sigma_{max} t} \ . \tag{4}$$

Then, we choose N electrons in a random manner and verify if any of them undergoes a collision. In order to do this we have to calculate collision probability from the following formula:

$$\mathcal{P}_{collision} = \frac{n_n \sigma(v_e) t}{\mathcal{P}_{max}} \tag{5}$$

and compare it with a random number $r \in [0, 1]$. The particle undergoes a collision only if $r \leqslant \mathcal{P}_{\text{collision}}$.

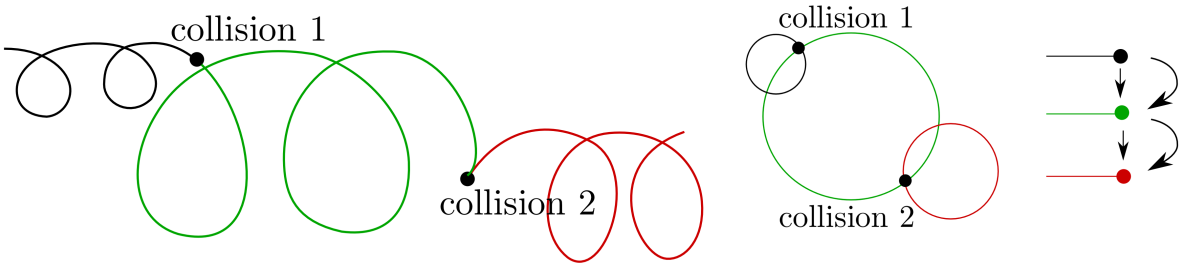

Figure 1: (left) Motion of an electron and its collisions as seen in the frame of reference of the thruster, (middle) in the the drifting frame and (right) its guiding center random walk representation.

B. Collisional random walk

The guiding center approximation implies that an electron is bound to a specific magnetic line unless it experiences a collision. After the collision, the position of its guiding center changes in a random-walk fashion (i.e. instantly). Henceforth we shall refer to this process as to a collisional random walk. Collisional random walk is best described in the x-y plane, perpendicular to the magnetic field line, as we assume that the electron guiding center just before and shortly after the collision is located on this surface. Figure 1 shows the graphical interpretation of the random walk of guiding centers.

The main challenge in modeling collisional random walk is to properly locate the position of the guiding center after the collision. For the case of a uniform magnetic field, the guiding center might be defined geometrically as a center of electron rotation. However, the simple definition of the guiding center has to be refined when guiding center drifts emerge, caused either by the magnetic field gradients or by the presence of an external force (e.g. due to the electric field). When the guiding center is subject to a drift, the electron follows a cycloidal trajectory. The geometrical definition of the guiding center could then be redefined to mean an average position of the electron over a single gyroperiod. However, this definition does not enable efficient calculation of the position of the guiding center by a numerical model.

Since the discussed cross-field electron transport model is one-dimensional and we are only interested in calculating x_{gc}, the guiding center shall hereafter be defined as the point, where

$$|v_x(x_{gc})| = max(|v_x(x)|) = \widetilde{v}_\perp \ . \tag{6}$$

Henceforth the $\widetilde{}$ symbol shall identify the values calculated in the frame of the guiding center. The aforementioned definition of the guiding center is equivalent to the following relation:

$$v_y(x_c) = -\frac{E(x_c)}{B(x_c)} \ . \tag{7}$$

For computational efficiency, an energy conserving method of searching for x_{gc} is proposed, using the following constants of motion [6]:

$$c = v_x^2 + v_y^2 + \frac{2q_e}{m_e}\Phi \tag{8}$$

$$d = v_y + \frac{q_e}{m_e}A \ . \tag{9}$$

Here Φ is the electric field potential and A is the magnetic field potential.

Using Eqs. (8) - (9) we find the following relation:

$$v_x^2 = c - \frac{2q_e}{m_e}\Phi - \left(d - \frac{q_e}{m_e}A\right)^2 \ , \tag{10}$$

which enables us to find x_{gc} as the point where RHS reaches a maximum, solving the following equation:

$$\frac{E}{B} - \frac{q_e}{m_e}A + d = 0 \ . \tag{11}$$

Equation (11) could also be obtained by substituting v_y in Eq. (9) by $-\frac{E}{B}$ of Eq. (7).

Detailed description of the algorithm for finding new guiding center position is presented in the Appendix. Having the new position of the guiding center enables us to calculate the distance traveled by the guiding center during a collision. This information is important for computing the overall cross-field electron transport.

II. Cross-field electron transport

A. Method 1: generalized Ohm's law

The first approach towards calculating the electric field perpendicular to the magnetic field that we investigated was based on the generalized Ohm's law. This seemed to be a natural choice since the electric field parallel to the magnetic field is calculated in this manner.

Ohm's law in the following form was used:

$$q_e E_\perp = \frac{1}{n_i}\frac{\partial\left(n_i k_B T_{e_\perp}\right)}{\partial x} + m_e \left\langle \frac{\omega_c^2}{\nu_e} v_x \right\rangle \ . \tag{12}$$

The method is successfully used in hybrid codes, which treat electrons as a fluid [7,8]. However, the kinetic description of electron motion revealed correlation between ν_e and v_x, which makes the calculation of $\left\langle \frac{\omega_c^2}{\nu_e} v_x \right\rangle$ cumbersome. Contrary to the hybrid codes of Refs. [7] & [8] we compute electron collision frequency directly from the Monte Carlo collision solver. Anomalous electron transport was not accounted for but could be in principle included as an additional collisional process. Numerical experiments have shown us that disregarding the correlation between ν_e and v_x resulted in overpredicting the value of the electric field. Since v_x was calculated based on guiding centers' jumps and not on their motion under the electric field, there was considerable numerical noise associated with this method, which is why the code had problems with retaining stability.

B. Method 2: Gauss's law

Because of the difficulties that appeared during the implementation of the method described in Sec. A, we decided to compute $E_\perp$ by solving Gauss's law in the direction perpendicular to the magnetic field:

$$\nabla \cdot \mathbf{E} = \frac{\rho}{\varepsilon_0} \ . \tag{13}$$

Solving equation (13) is equivalent to solving Poisson equation and so it imposes in principle identical limits on both spatial and temporal resolution of the model.

In the case of the guiding center description, however, the plasma oscillation is absent and the timestep is not constrained by the plasma frequency, but rather by the electron collision frequency. Therefore, the stability criterion for time discretization is significantly relaxed compared to standard PIC-Poisson simulations and we can use $dt >> \frac{1}{\omega_{pe}}$.

Since Gauss's law stands here merely as a computationally convenient approximation of the quasineutrality condition, physical correctness of quantities such as plasma frequency or Debye length is not mandated. This is why the upper limit on the grid spacing may be artificially increased by increasing the vacuum permittivity in order to ensure that the Debye length is everywhere of the order of the grid spacing.

Since the 1D code developed by Miedzik et al. [1,2] presumes quasineutrality, we have to make sure that it is also satisfied in our code.

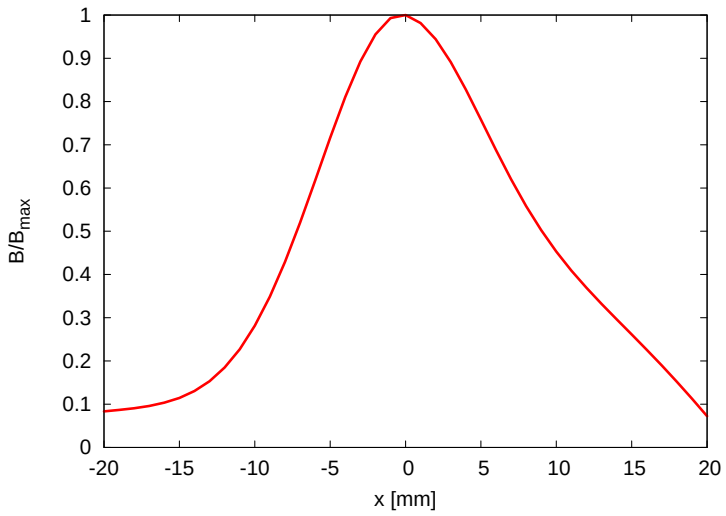

Figure 2: Magnetic field profile.

III. Results

In this section we present results obtained with a one-dimensional model along the Hall thruster channel. The computational domain is divided into 40 cells and covers a distance of 4 cm. Xenon is fed through the anode with a constant mass flow rate. We assume constant electric field on the anode $E_A = -9000$ V/m. The profile of the magnetic field is shown in Fig. 2. The vacuum permittivity was increased 500 times compared to the real value. Figure 4 shows that quasineutrality is still at an acceptable level.

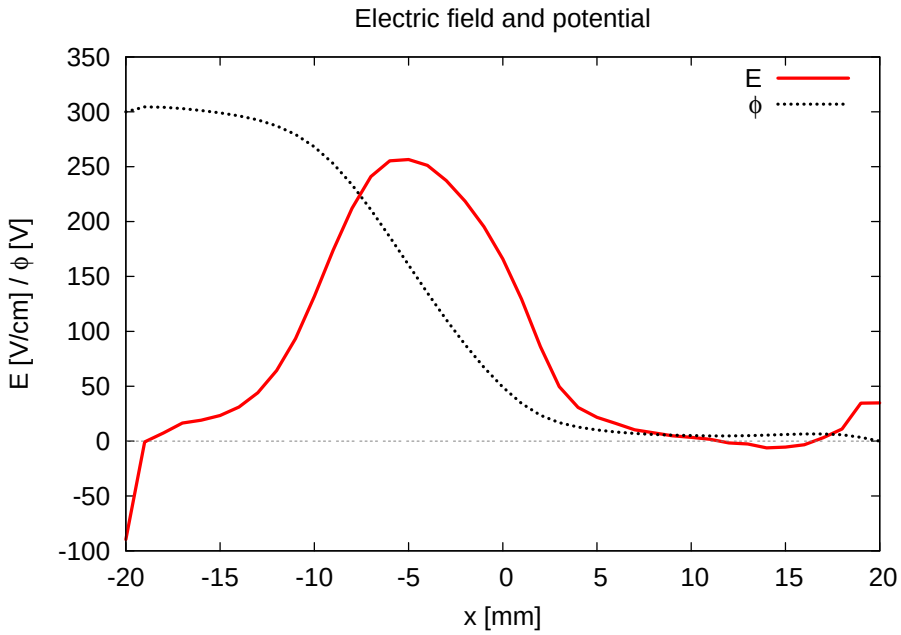

Figure 3: Electric field and potential.

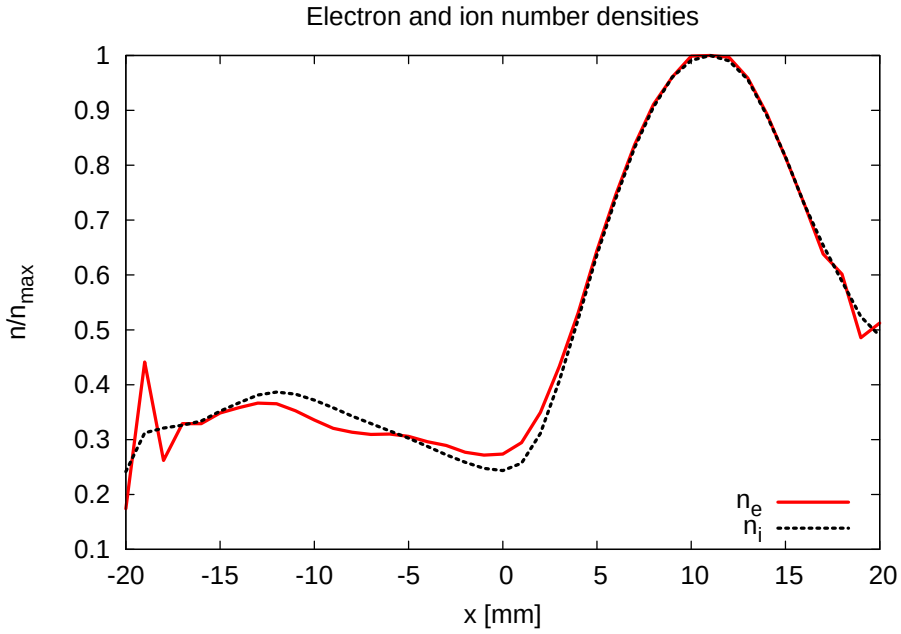

Figure 4: Electron and ion number densities.

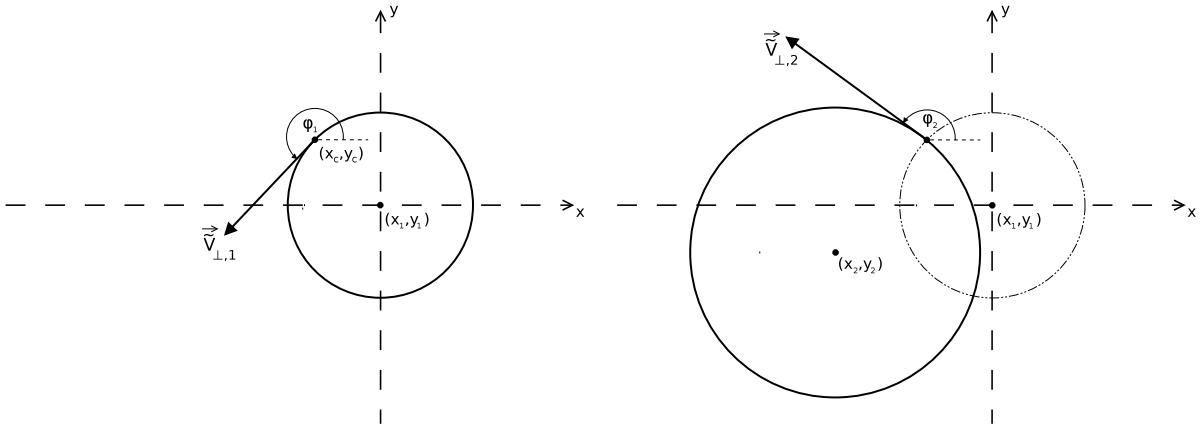

(a) Electron orbit prior to collision.

(b) Electron orbit after the collision.

Figure 5: Sample scattering scenario.

IV. Conclusion

We have investigated various aspects of a cross-field transport of electrons described in the frame of the guiding center approximation. The fact that electrons are at rest in the drifting frame until they experience a collision makes the problem considerably different from the one solved by conventional PIC-Poisson codes which integrate electron trajectories.

First of all, the plasma oscillations disappear from the system, which enables the use of $dt >> \frac{1}{\omega_{pe}}$. Since the cyclotron motion is not resolved, the limitation on dt is further relaxed, allowing for $dt >> \frac{1}{\omega_c}$. The Courant-Friedrichs-Levy (CFL) condition for electrons is inapplicable since electrons move in a random walk manner (i.e. instantly) and, notwithstanding the timestep, may jump through more than one cell in a given timestep. The CFL condition for ions does limit the timestep for the parameters presented in Sec. III to about $dt \sim 10^{-8}$ s. However, we have discovered that a more constraining condition concerning dt exists and is connected with the electron collision frequency. For simulations described in Sec. III the use of $dt \sim 10^{-8}$ s usually led to significant numerical noise caused by a large number of collisions occurring during a single timestep. We have not postulated any condition relating dt to collision frequency, but a trial-error approach suggests that $dt \sim 10^{-9}$ s provides adequate stability.

The fact that plasma oscillations are absent makes it possible to increase the value of the vacuum permittivity without altering any of the characteristic frequencies of the system. The increased value of the vacuum permittivity results in a longer Debye length, allowing for the use of a coarser computational grid.

The next step shall be to transfer the one-dimensional cross-field electron transport solver into a two-dimensional, realistic thruster geometry. Results presented in Sec. III show that using the Gauss's law to calculate the electric field perpendicular to the magnetic field retains quasineutrality even for an increased value of the vacuum permittivity, a necessary condition to successfully couple this method in a set of 1D simulations which presume quasineutrality.

Appendix

Figure 5 presents a sample scattering scenario that depicts the following algorithm:

1. PRIOR TO COLLISION

   i. Determine the position of the electron's guiding center (x_1, y_1) and its velocities in the frame of reference of the guiding center, $\widetilde{v}_{\parallel,1}$ and $\widetilde{v}_{\perp,1} = \sqrt{\frac{2B\mu}{m_e}}$.

   ii. Choose a random gyrophase, $\phi_1 \in [0, 2\pi)$.

iii. Calculate components of the perpendicular velocity in the frame of the guiding center:

$$\begin{cases} \widetilde{v}_{x,1} = \widetilde{v}_{\perp,1} \cos\phi_1 \\ \widetilde{v}_{y,1} = \widetilde{v}_{\perp,1} \sin\phi_1 \ . \end{cases} \tag{14}$$

iv. Transform velocities to the frame of reference of the thruster:

$$\begin{cases} v_{\parallel,1} = \widetilde{v}_{\parallel,1} \\ v_{x,1} = \widetilde{v}_{x,1} \\ v_{y,1} = \widetilde{v}_{y,1} - \frac{E(x_1)}{B(x_1)} \ . \end{cases} \tag{15}$$

v. Calculate perpendicular velocity in the frame of the thruster, $v_{\perp,1} = \sqrt{v_{x,1}^2 + v_{y,1}^2}$ and total velocity prior to collision, $v_1 = \sqrt{v_{\parallel,1}^2 + v_{\perp,1}^2}$.

vi. Calculate constants of motion of Eqs. (8) - (9) at point (x_1, y_1):

$$\begin{cases} c_1 = \widetilde{v}_{\perp,1}^2 + \left(-\frac{E(x_1)}{B(x_1)}\right)^2 + \frac{2q_e}{m_e}\Phi(x_1) \ , \\ d_1 = -\frac{E(x_1)}{B(x_1)} + \frac{q_e}{m_e}A(x_1) \ . \end{cases} \tag{16}$$

vii. Having c_1 and d_1 determine Φ and A at the collision point (x_c, y_c):

$$\begin{cases} \Phi(x_c) = \frac{m_e}{2q_e}\left(c_1 - \left(v_{x,1}^2 + v_{y,1}^2\right)\right) \ , \\ A(x_c) = \frac{m_e}{q_e}\left(d_1 - v_{y,1}\right) \ . \end{cases} \tag{17}$$

2. AFTER THE COLLISION

i. Calculate total velocity after the collision, v_2 (in the case of elastic interaction, the electron energy is conserved and v_2 is simply equal to v_1).

ii. Choose θ and ϕ_2 such that a random scattering solid angle is equiprobable:

$$\begin{cases} \theta \ \in [0, \pi) & \text{with reference to } z \text{ axis} \\ \phi_2 \in [0, 2\pi) & \text{with reference to } x \text{ axis} \ . \end{cases} \tag{18}$$

iii. Calculate velocities in the frame of the thruster:

$$\begin{cases} v_{\parallel,2} = v_2 \cos\theta \\ v_{x,2} = v_2 \sin\theta \cos\phi_2 \\ v_{y,2} = v_2 \sin\theta \sin\phi_2 \ . \end{cases} \tag{19}$$

iv. Calculate constants of motion of Eqs. (8) - (9):

$$\begin{cases} c_2 = v_{x,2}^2 + v_{y,2}^2 + \frac{2q_e}{m_e}\Phi(x_c) \\ d_2 = v_{y,2} + \frac{q_e}{m_e}A(x_c) \ . \end{cases} \tag{20}$$

v. Find the new guiding center position, defined as a point, where v_x reaches maximum and $v_y = -\frac{E}{B}$ by solving Eq. (11):

$$\frac{E(x_2)}{B(x_2)} - \frac{q_e}{m_e}A(x_2) + d_2 = 0 \ . \tag{21}$$

vi. Transform velocities to the frame of the new guiding center:

$$\begin{cases} \widetilde{v}_{\parallel,2} = v_{\parallel,2} \\ \widetilde{v}_{x,2} = v_{x,2} \\ \widetilde{v}_{y,2} = v_{y,2} + \frac{E(x_2)}{B(x_2)} \ . \end{cases} \tag{22}$$

Acknowledgments

D. Daniłko is thankful to Snecma for the sponsorship of his PhD thesis and to J. Miedzik for sharing his code as well as providing invaluable support all along. This work had a financial support from the French Research Group "Propulsion par Plasma dans l'Espace" (GDR 3161 CNRS/CNES/SNECMA/Universités).

References

[1]Miedzik, J. and Barral, S., "Electron Guiding Center Modeling for Hall Thruster Simulations," *Proc. 31st International Electric Propulsion Conference*, No. 09-069, The Electric Rocket Propulsion Society, Worthington, OH, Ann Arbor, MI, 2009.

[2]Miedzik, J., Barral, S., and Zurbach, S., "Study of Plasma Confinement by Magnetic Fields in Hall Thrusters using Quasi-Neutral PIC Modeling," *Proc. 32nd International Electric Propulsion Conference*, No. 11-238, The Electric Rocket Propulsion Society, Worthington, OH, Wiesbaden (Germany), 2011.

[3]Fuchs, V. and Gunn, J. P., "On the Integration of Equations of Motion for Particle-In-Cell Codes," *J. Comput. Phys.*, Vol. 214, 2006, pp. 299.

[4]Lampe, M., Joyce, G., Manheimer, W. M., and Slinker, S. P., "Quasi-Neutral Particle Simulation of Magnetized Plasma Discharges: General Formalism and Application to ECR Discharges," *IEEE. Trans. Plasma Sci.*, Vol. 26, 1998, pp. 1592.

[5]Koura, K., "Null-collision technique in the direct-simulation Monte Carlo method," *Phys. Fluids*, Vol. 29, No. 11, 1986, pp. 3509.

[6]Clemmow, P. C. and Dougherty, J. P., *Electrodynamics of Particles and Plasmas*, Addison-Wesley Series in Advanced Physics, Addison-Wesley Pub. Co., 1969.

[7]Fife, J. M., *Hybrid-PIC Modeling and Electrostatic Probe Survey of Hall thrusters*, Ph.D. thesis, Massachusetts Institute of Technology, 1998.

[8]Mikellides, I. G., Katz, I., Hofer, R. R., and Goebel, D. M., "Hall-Effect Thruster Simulations with 2-D Electron Transport and Hydrodynamic Ions," *Proc. 31st International Electric Propulsion Conference*, No. 09-114, The Electric Rocket Propulsion Society, Worthington, OH, Ann Arbor, MI, 2009.